Journal of Applied Polymer Science

Electrospun plasma-modified chitosan/poly(ethylene terephthalate)/ferrocenyl-substituted *N*-acetyl-2-pyrazoline fibers for phosphate anion sensing

Neslihan Nohut Maslakci,[1] Esin Eren,[2] Seda Demirel Topel,[3] Gunseli Turgut Cin,[3] Aysegul Uygun Oksuz[1]

[1]Department of Chemistry, Faculty of Arts and Science, Suleyman Demirel University, Isparta 32260, Turkey
[2]Hydrogen Technologies Research and Application Center, Suleyman Demirel University, Isparta 32260, Turkey
[3]Department of Chemistry, Faculty of Science, Akdeniz University, Antalya 07058, Turkey
Correspondence to: A. U. Oksuz (E-mail: ayseguluygun@sdu.edu.tr)

ABSTRACT: Two ferrocenyl-substituted *N*-acetyl-2-pyrazolines, *N*-acetyl-3-(2-furyl)-5-ferrocenyl-2-pyrazoline (Fc-1) and *N*-acetyl-3-(2-thienyl)-5-ferrocenyl-2-pyrazoline (Fc-2) electrospun fibers, were produced in the presence of plasma-modified chitosan (PMCh)/poly(ethylene terephthalate) (PET) supporting polymers with an electrospinning method. The morphological and chemical characterizations of the PMCh/PET/Fc-1 and PMCh/PET/Fc-2 electrospun fibers were determined by scanning electron microscopy coupled with energy-dispersive X-ray spectroscopy analysis. Thermogravimetric analysis results indicated the presence of ferrocene within the PMCh/PET nanofibers. The electrochemical behavior of the PMCh/PET/Fc-1 and PMCh/PET/Fc-2 electrospun fibers were investigated by cyclic voltammetry measurements based on the ferrocene/ferrocenium redox couple. The new PMCh/PET/Fc-1 and PMCh/PET/Fc-2 electrospun fibers aggregated on the indium tin oxide were used for phosphate anion sensing. The highest oxidation peak currents were observed for the PMCh/PET/Fc-1 electrospun fibers at about 0.56 V in 0.1*M* phosphate buffer. © 2015 Wiley Periodicals, Inc. J. Appl. Polym. Sci. **2016**, *133*, 43344.

KEYWORDS: blends; electrochemistry; electrospinning; fibers; inorganic polymers

Received 1 September 2015; accepted 12 December 2015
DOI: 10.1002/app.43344

INTRODUCTION

Ferrocene is a well-known mediator because of its diverse properties, such as its reversibility, unique redox behavior, thermal stability, and low price.[1,2] Recently, ferrocene and its derivatives have been shown to have interdisciplinary activities ranging from materials science to biological assays.[3–5] It was reported that most various ferrocenyl-substituted compounds, such as condensed imidazoles,[6,7] triazoles,[8–11] guanidine,[12] oxazoles,[13,14] and pyrimidines,[15–17] have attracted substantial interest because of their widespread applications in the fields of medicine,[15,18,19] supramolecular chemistry,[20,21] materials science,[22,23] and sensors.[24] On the other hand, pyrazolines have propensities as blue-light-emitting fluorescent agents with high quantum yields[5,25–28] and hole-transport tendencies.[5,29–32] In recent years, it was reported that some ferrocenyl pyrazoline derivatives exhibited important pharmacological and optical properties.[5,19,33–36] Applications of ferrocenyl pyrazoline derivatives in materials science[5,19,36] could be improved by the preparation of electrospun fibers; this depends on the increased surface area.

Chitosan and ferrocene hybrids have been used to obtain a functionalized matrix in electrochemical biosensors for immobilizing assorted enzymes, such as glucose oxidase. The covalent linking of ferrocene to chitosan can prevent leakage in the entrapment of the mediator.[37] Moreover, ferrocene groups increase the electron-transfer process between the electrode surface and the immobilized biocatalyst; this allows one to obtain more sensitive and stable biosensors.[37,38] Ferrocene derivatives, including aldehyde groups, can simply react with the NH_2 group of chitosan to give a Schiff base, and then, the reduction via $NaCNBH_3$ occurs. Because of the hydrophobic properties of the ferrocenyls, the number of redox active sites in the polymer is limited. This problem was dissolved via functionalized polysiloxane with a chitosan composite of ferrocene; this indicated a greater transport rate in the aqueous condition.[38]

Electrospinning is a novel and efficient method for producing ultrathin fibers from a wide range of polymer materials. A characteristic property of the electrospinning process is the excessively rapid formation of the nanofiber structure on a

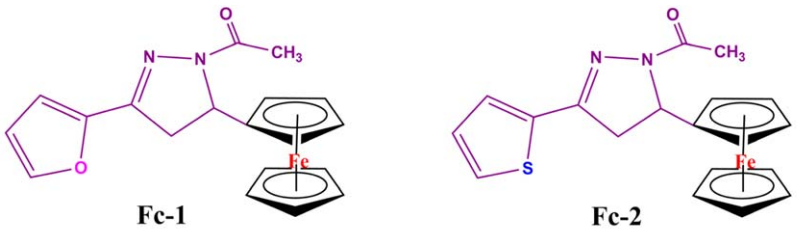

Figure 1. Chemical structures of the synthesized ferrocenyl *N*-acetylated-2-pyrazolines. [Color figure can be viewed in the online issue, which is available at wileyonlinelibrary.com.]

millisecond scale. Other remarkable properties of electrospinning are its enormous material elongation rate on an order of 1000 s^{-1} and a cross-sectional area reduction on an order of 10^5–10^6; these have been shown to affect the orientation of the structural elements within the fiber.[39] Moreover, the polymer solutions are very important for producing electrospun fibers under various parameters (e.g., solution concentration, voltage).[40]

Recent scientific research has focused on the study of both ferrocene-derived nanofibers and chitosan nanofibers via electrospinning technology.[41–46] To the best of our knowledge, chitosan nanofibers containing ferrocenyl-substituted *N*-acetyl-2-pyrazoline derivatives prepared via electrospinning have not been reported up to this point.

In our previously published articles, we reported the modification of the chitosan surface via a radio-frequency hydrazine plasma.[46,47] In this way, the properties of chitosan were successfully improved through an increase in the free amino group function. Because of enhanced functionality of the group with close packing between the chitosan chains at the molecular level, this leads to increased chitosan chain mobility and chain scission.[47] Therefore, in this study, radio-frequency hydrazine plasma-modified chitosan (PMCh) was used to obtain fibers in the presence of poly(ethylene terephthalate) (PET).

The nanofibers of PMCh and ferrocenyl-substituted *N*-acetyl-2-pyrazoline derivatives were prepared via electrospinning methods in the presence of PET as a supporting material. The obtained nanofibers were characterized via scanning electron microscopy (SEM)–energy-dispersive X-ray spectroscopy (EDX) analysis and thermogravimetric analysis (TGA) methods. Cyclic voltammetry (CV) measurements were carried out to prove the presence of ferrocene units in the fiber structures and to emphasize the anion sensibility of the electrospun fibers with phosphate anions.

EXPERIMENTAL

Materials and Methods

Low-molecular-weight chitosan (deacetylation degree $\geq$ 75%) was purchased from Aldrich. The molecular weight was approximately 50,000–190,000 Da on the basis of the viscosity. PET (weight-average molecular weight = 30.000) was supplied from Scientific Polymer. Trifluoroacetic acid (TFA; 99%) was purchased from Aldrich and was used as supplied. Dichloromethane (DCM) was purchased from Merck (99.8%), and sodium perchlorate ($NaClO_4$; Aldrich) was used as a supporting electrolyte for the CV experiments. Buffer solutions (pH 7.4) were prepared with Na_2HPO_4 (anhydrous, Aldrich) and $NaH_2PO_4{\cdot}H_2O$ (Aldrich).

Two ferrocenyl-substituted *N*-acetyl-2-pyrazolines, *N*-acetyl-3-(2-furyl)-5-ferrocenyl-2-pyrazoline (Fc-1) and *N*-acetyl-3-(2-thienyl)-5-ferrocenyl-2-pyrazoline (Fc-2), were synthesized according to previous studies.[36,48] The chemical structures of the used ferrocenyl *N*-acetylated-2-pyrazoline derivatives are shown in Figure 1.

Formation of the PMCh/PET/Fc-1 and PMCh/PET/Fc-2 Electrospun Fibers

For electrospinning, PMCh (0.5 g) was dissolved in TFA (8 mL). A concentration of 15 wt % PET was dissolved in TFA (1.4 mL) and DCM (1.4 mL), respectively. To obtain a homogeneous solution of the PMCh/PET, a binary mixture with a volume ratio of 1:1 was prepared under constant stirring at room temperature for 24 h.[44,45]

The ferrocenyl-substituted *N*-acetyl-2-pyrazoline derivatives, Fc-1 (3.31×10^{-4} mol) and Fc-2 (3.17×10^{-4} mol), were dissolved in DCM (1 mL) and were added to the obtained PMCh/PET solution at volume ratios of 1:1. The mixtures were stirred at room temperature for 24 h. Green homogeneous solutions were obtained.

A homemade electrospun system was built and used for fiber production. A custom-made, high-voltage, direct-current converter (EMCO 4300) was biased with a direct-current power supply.[42,46] The prepared electrospinning solution was loaded into a plastic syringe equipped with a stainless steel needle and with a volume of 2 mL. The following constant system parameters were used for the electrospinning process: an applied voltage of 15 kV, a solution flow rate of 10 μL/h, and a tip-to-collector distance of 5 cm.

Characterization of the PMCh/PET/Fc-1 and PMCh/PET/Fc-2 Electrospun Fibers

The electrospun fibers of PMCh/PET/Fc-1 and PMCh/PET/Fc-2 were coated onto an indium tin oxide (ITO) glass substrate to perform the CV measurements. Redox behaviors of the PMCh/PET/Fc-1 and PMCh/PET/Fc-2 electrospun fibers between −0.5 and 1.0 V were determined with a Gamry 300 model potentiostat with a three-electrode system at a scan rate of 50 mV/s.

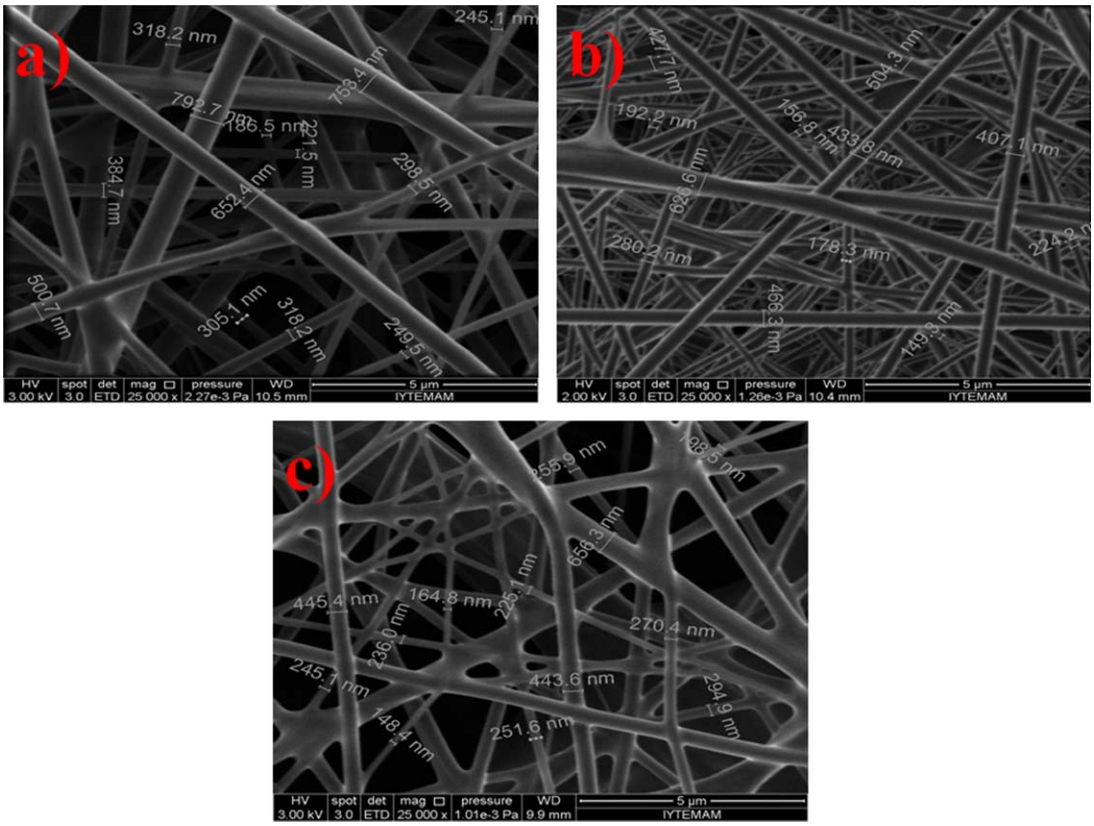

Figure 2. SEM images of the electrospun fibers: (a) PMCh/PET, (b) PMCh/PET/Fc-1, and (c) PMCh/PET/Fc-2. [Color figure can be viewed in the online issue, which is available at wileyonlinelibrary.com.]

The electrochemical sensing of the PMCh/PET/Fc-1 and PMCh/PET/Fc-2 electrospun fibers of phosphate anions was investigated with CV measurements in 0.1*M* $NaClO_4$ with changing concentrations of phosphate buffer (PB; $NaH_2PO_4{\cdot}H_2O$).

The synthesized electrospun fibers of PMCh/PET/Fc-1 and PMCh/PET/Fc-2 were analyzed with SEM–EDX (Quanta 250 scanning electron microscope and Phillips XL-30S FEG microscope). TGA measurements (Perkin–Elmer model, Beaconsfield, Bucks HP91QA, United Kingdom) of the PMCh/PET/Fc-1 and PMCh/PET/Fc-2 electrospun fiber samples were performed by heating at a rate of 10°C/min in the presence of an N_2 atmosphere from 25 to 900°C.

RESULTS AND DISCUSSION

PMCh/PET/Fc-1 and PMCh/PET/Fc-2 Electrospun Fibers

The TFA/DCM system, which is one of the most promising solvent systems[49] for the electrospinning of homogeneous PMCh/PET electrospun fibers, was also used to dissolve Fc-1 and Fc-2. Between the pyrazoline derivatives, $C_{19}H_{18}N_2O_2Fe$ (Fc-1) and $C_{19}H_{18}N_2OSFe$ (Fc-2), and the chitosan $(C_6H_{11}NO_4)_n$, intermolecular interactions such as hydrogen bonds could occur. Chitosan protonated to NH_3^+ in acid media. This could have been due to hydrogen-bonding interactions between the NH_3^+ group of chitosan molecules and the C═O groups of Fc-1, Fc-2, and PET molecules.[50]

Before we could obtain ideal (uniform, submicrometer and/or micrometer scaled) PMCh/PET/Fc-1 and PMCh/PET/Fc-2 electrospun fibers, first, the optimum solution concentration of the compounds was determined. The most suitable PMCh/PET electrospun fibers were obtained at a concentration of 15 wt % PET with a tip-to-collector distance of 5 cm, a solution flow rate of 10 µL/h, and a voltage of 15 kV. The PMCh/PET electrospun fibers were also observed at a volume ratio of 1:1.

SEM images of the PMCh/PET, PMCh/PET/Fc-1, and PMCh/PET/Fc-2 electrospun fibers are shown in Figure 2(a–c), respectively. PET used as a supporting polymer was capable of providing electrospun fiber formation. The PMCh/PET electrospun fibers were deposited on to the ITO electrode surface, and the diameters of the nanofibers were measured in the range of 220 and 800 nm. In the ferrocenyl-substituted *N*-acetyl-2-pyrazoline derivative (Fc-1 and Fc-2) loaded PMCh/PET electrospun fibers, the effects of the Fc-1 and Fc-2 loadings on the morphologies and diameters of the electrospun fibers were investigated.

In the electrospun fibers, the presence of the Fc-1 and Fc-2 components were confirmed by the EDX results (Table I). The average diameters of the fibers are also given as the means plus or minus the standard deviations in Table I. Iron (Fe) could be used as an indicator for the existence of ferrocene in the fiber structure. Sulfur (S) atoms were solely attributed to the Fc-2 structure in the PMCh/PET electrospun fibers (see Table I for the structure of the PMCh/PET/Fc-2 electrospun fibers), and the presence of the S peak in the EDX spectra indicated the successful incorporation of Fc-2 in the nanofibers through electrospinning. To examine the distribution of Fc-1 and Fc-2 on the

Table I. Summary of the EDX Results and Average Diameters of the PMCh/PET, PMCh/PET/Fc-1, and PMCh/PET/Fc-2 Electrospun Fibers

	wt %					
Fiber sample	C	O	N	S	Fe	Average diameter of fibers (nm)
PMCh/PET	67.79	31.69	0.52	—	—	402.0 ± 196.2
PMCh/PET/Fc-1	65.17	30.56	1.14	—	3.13	337.2 ± 152.9
PMCh/PET/Fc-2	67.39	28.50	1.42	0.80	1.89	295.0 ± 135.2

nanofibers, S (blue spots) and Fe (red spots) mapping is shown in Figure 3(a,b). In Figure 3(a,b), the increases in the number of red spots in the fibers of Fc-1 and Fc-2 confirmed the dispersion of ferrocene throughout the PMCh/PET/Fc-1 and PMCh/PET/Fc-2 electrospun fibers.

Generally, the conductivity of a polymer solution has a significant effect on the electrospun fiber morphology and jet formation, as known from many published articles. The solution conductivity is determined on the basis of the polymer type, solvent type, availability of ionizable salts, and effect of conductivity groups.[51] During electrospinning, it has been found that with a decrease in the electrical conductivity of the polymer solution, there is a significant increase in the diameter of the electrospun nanofibers, whereas a high conductivity in the polymer solution results in a significant decrease in the diameter of the electrospun fibers.[51]

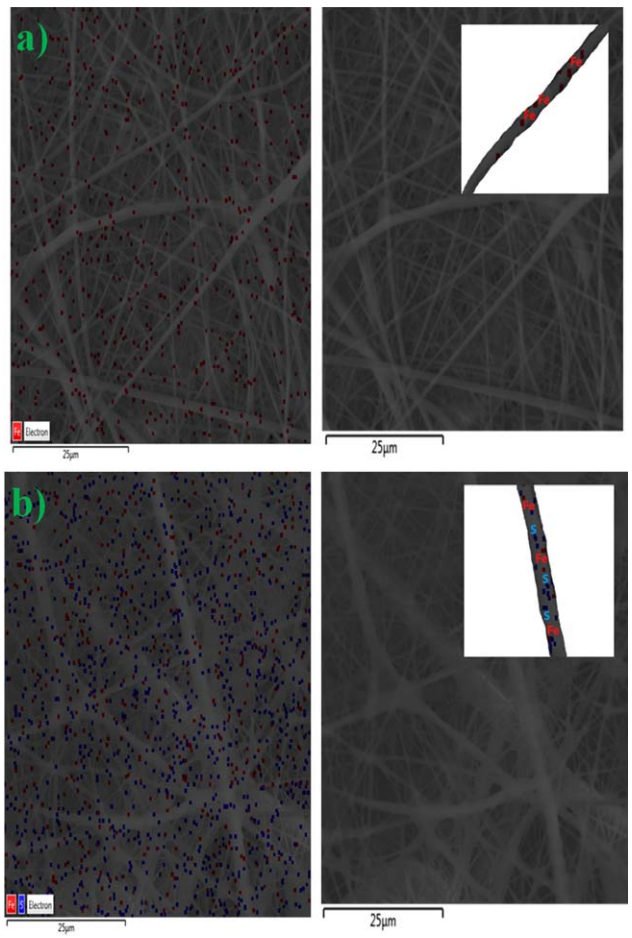

Figure 3. Comparison of the S and Fe mapping in electrospun fibers: (a) PMCh/PET/Fc-1 and (b) PMCh/PET/Fc-2. [Color figure can be viewed in the online issue, which is available at wileyonlinelibrary.com.]

Thermal Analysis of the PMCh/PET/Fc-1 and PMCh/PET/Fc-2 Electrospun Fibers

As shown in Figure 4, the degradation process of the PMCh/PET, PMCh/PET/Fc-1, and PMCh/PET/Fc-2 electrospun fibers were investigated with TGA from 25 to 900°C in nitrogen gas. Because of the evaporation of adsorbed water or moisture, the TGA results of all of the samples showed a first weight loss of 5–10% before approximately 100°C.[41] The TGA curves of Fc-1 and Fc-2 each showed one decomposition stage between approximately 130 and 400°C, as shown in Figure 4. This was due to the thermal decomposition of these compounds. The residual amounts at 900°C obtained were 4.9 and 21.7 wt % for the Fc-1 and Fc-2 powders, respectively. It is well known from the previous research that both of the compounds have similar degradation processes, but Fc-2 is more resistant to decomposition.[36] The PMCh/PET electrospun fibers showed a weight loss with two steps. The first maximum weight loss at 275°C showed the degradation of the PMCh chain. This degradation temperature was lower than that of the unmodified chitosan, as is known from our previous studies, because of the increased chitosan chain mobility and chain scission via plasma treatment.[47,52] The second degradation temperature, observed at approximately 415°C, corresponded to the degradation of the PET polymer backbone units.[53] With respect to the amount of residue at 900°C, the greatest weight loss was obtained for the PMCh/PET electrospun fibers.

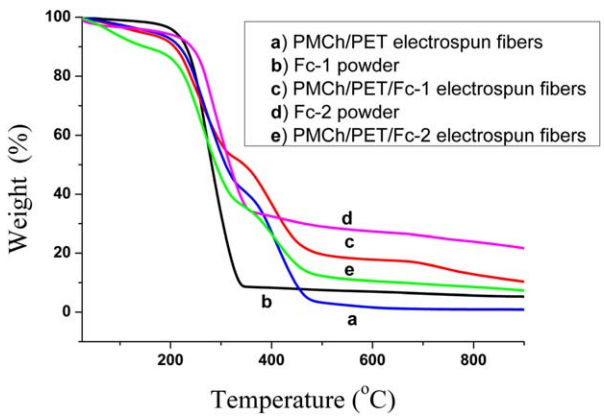

Figure 4. TGA thermograms of the (a) PMCh/PET electrospun fibers, (b) Fc-1 powder, (c) PMCh/PET/Fc-1 electrospun fibers, (d) Fc-2 powder, and (e) PMCh/PET/Fc-2 electrospun fibers. [Color figure can be viewed in the online issue, which is available at wileyonlinelibrary.com.]

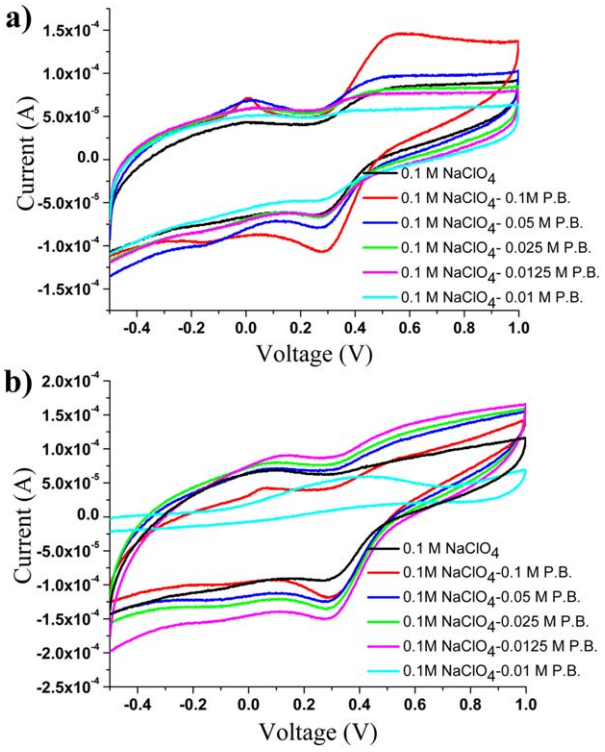

Figure 5. Cyclic voltammograms of the (a) PMCh/PET/Fc-1 and (b) PMCh/PET/Fc-2 electrospun fibers obtained for different concentrations of PB and 0.1*M* $NaClO_4$ at a scan rate of 50 mV/s. [Color figure can be viewed in the online issue, which is available at wileyonlinelibrary.com.]

The trend of the degradation curves of the PMCh/PET electrospun fibers containing ferrocenyl pyrazoline derivatives was similar to that of the PMCh/PET electrospun fibers. In the PMCh/PET electrospun fibers weight loss curve, it was evident that the first degradation step was due to both PMCh and ferrocenyl pyrazoline derivatives, and the second one was due to the PET polymer backbone. TGA was used to record the weight loss of all of the fibers. Moreover, the aim of the TGA measurements was to determine amount of Fe in the PMCh/PET electrospun nanofibers. The residual amounts of the PMCh/PET/Fc-1 and PMCh/PET/Fc-2 electrospun fibers at 900°C were determined as 10 and 7 wt %, respectively. The amount of Fe in the PMCh/PET/Fc-1 electrospun nanofibers was higher than that of the PMCh/PET/Fc-2 electrospun nanofibers. This result was consistent with the EDX results.[42]

Electrochemical Studies

The electrochemical characterization of the PMCh/PET/Fc-1 and PMCh/PET/Fc-2 electrospun fibers were performed by means of CV in 0.1*M* $NaClO_4$ and PB at different concentrations [Figure 5(a,b)] with a three-electrode cell consisting of an ITO working electrode, a platinum wire auxiliary electrode, and Ag/AgCl as the reference electrode at a scan rate of 50 mV/s. Table II summarizes the redox potential data of the PMCh/PET/Fc-1 and PMCh/PET/Fc-2 electrospun fibers.

Cyclic voltammograms of ferrocene and its derivatives are known to exhibit regular waves corresponding to the reversible ferrocene/ferrocenium redox couple.[54,55]

Therefore, the oxidation and reduction peaks were measurements related to the ferrocene components in the electrospun fiber films. On the other hand, the PMCh/PET electrospun fibers loaded with ferrocene component exhibited a sharper CV area than that of the unloaded PMCh/PET electrospun fibers. This situation could have been related to the presence of well-dispersed ferrocene compounds; this led to enhancement of the connectivity and the electrochemical utilization of the PMCh/PET electrospun fibers during the charge/discharge process. The performance of the electrospun fibers was strongly influenced by the presence of ferrocene in the fiber structures. It is apparent from Figure 5(a,b) that the peak current for the PMCh/PET/Fc-1 and PMCh/PET/Fc-2 electrospun fibers was higher than those of the unloaded PMCh/PET electrospun fibers; this suggested that the presence of ferrocene compounds improved its activity.

CV of the PMCh/PET/Fc-1 and PMCh/PET/Fc-2 electrospun fiber coated ITO electrode showed anodic/cathodic peaks because of the ferrocene/ferrocenium centers of the Fe, which were covalently bound to the insoluble polymer skeleton.

The highest peak currents were observed for the PMCh/PET/Fc-1 electrospun fibers at about 0.56 V in 0.1*M* PB [Figure 5(a)]. The PMCh/PET/Fc-1 and PMCh/PET/Fc-2 electrospun fibers showed electroactivity and the shifting of peak potentials in PB prepared at different concentrations (Table II).

The anion sensitivity measurements of the PMCh/PET/Fc-1 and PMCh/PET/Fc-2 electrospun fibers on ITO were made in the range 0.1–0.01*M* PB. The reduction current values for the PMCh/PET/Fc-1 electrospun fibers were monitored as a function of the phosphate concentration, and a linear decrease in the current

Table II. Peak Potentials of the PMCh/PET/Fc-1 and PMCh/PET/Fc-2 Electrospun Fibers with Various PB Concentrations in 0.1*M* $NaClO_4$

		PB concentration					
Fiber sample	Potential	—	0.1*M*	0.05*M*	0.025*M*	0.0125*M*	0.01*M*
PMCh/PET/Fc-1	E_{oxd} (V)	0.50	0.56	0.49	0.47	0.41	0.37
PMCh/PET/Fc-2		0.54	0.53	0.53	0.54	0.54	0.55
PMCh/PET/Fc-1	E_{red} (V)	0.25	0.28	0.26	0.26	0.28	0.27
PMCh/PET/Fc-2		0.27	0.29	0.29	0.29	0.30	—
PMCh/PET/Fc-1	$E_{1/2}$ (V)	0.37	0.42	0.37	0.36	0.34	0.32
PMCh/PET/Fc-2		0.40	0.41	0.41	0.41	0.42	—

E_{oxd}, oxidation peak potential; E_{red}, reduction peak potential at 25°C.

was observed from 0.1 to 0.01*M* PB [Figure 5(a)]. The reduction current values of the PMCh/PET/Fc-1 electrospun fibers were -1.06×10^{-4} and -4.62×10^{-5} A for 0.1 and 0.01*M* PBs at 0.28 V, respectively. In contrast, an exponential increase in the reduction current, which depended on the changes in the coated ITO surface with the PMCh/PET/Fc-2 electrospun fibers, was not observed from 0.1 to 0.01*M* PB [Figure 5(b)]. The reason for this result could have been the fact that the PMCh/PET electrospun fibers loaded nonhomogeneously and less with Fc-2. In addition, a more sensitive response of the PMCh/PET/Fc-1 electrospun fibers in the range 0.1–0.01*M* PB was also observed than that observed in the PMCh/PET/Fc-2 electrospun fibers, as shown in Figure 5(a,b).

We tested the electrochemical behavior of the ITO electrode modified with the PMCh/PET/Fc-1 electrospun fibers under the same conditions. The PCMh/PET/Fc-1 electrospun fiber coated electrode showed good reversible redox behavior at $E_{1/2} = 0.42$ V ($E_{1/2}$ identified as half-peak potential for a reversible redox couple at 25°C) for the 0.1*M* PB medium. It was clear that the reduction or oxidation peak potentials of the ITO electrode modified with the PMCh/PET/Fc-1 electrospun fibers were much smaller than those of the ITO electrode modified with the PMCh/PET/Fc-2 electrospun fibers. Furthermore, the $E_{1/2}$ (V) peak values of the PMCh/PET/Fc-2 electrospun fibers were higher than those of the PMCh/PET/Fc-1 electrospun fibers. Hendsbee *et al.*[56] investigated the substitution effects of furan and thiophene on the electrochemical properties. The onsets of oxidation and reduction for the furan-substituted compound obtained at 0.68 and −1.82 V, respectively, were slightly lower when compared to those of the thiophene-substituted compound. Thus, furan substitution led to an increase in the electron density of the small molecule. In this situation, the CV results confirmed that the PMCh/PET/Fc-1 electrospun fibers were more sensitive as anion sensors. The increase in the current values of the PMCh/PET/Fc-1 electrospun fibers was proportional to the increase in the PB concentration.

Moreover, the different potential shifts in CV showed that the PMCh/PET/Fc-1 and PMCh/PET/Fc-2 electrospun fibers provided various redox behaviors. The cathodic peaks for the PMCh/PET/Fc-1 fibers shifted to the right side of the voltammetric scale, whereas the anodic peaks of the PMCh/PET/Fc-2 fibers shifted to the right side of the voltammetric scale with increasing phosphate concentration [Figure 5(a,b)]. It is well known that negatively charged molecules can be incorporated into the $PVFc^{+}$ ClO_4^{-} film via anion exchange.[42,57] The results depend on the amount of ferrocene in the fiber structure with the phosphate concentration effect on the anodic and cathodic peak potentials. This state could be explained by the fact that Fe^{+} has a strong coordinating capacity.[42]

The faster, more reversible behavior of the PMCh/PET/Fc-1 and PMCh/PET/Fc-2 electrospun fibers could be explained by facile electron transport through Fc-1 and Fc-2 by the structural changes in the fibers caused by the introduction of chitosan. Chitosan is well known to be sensitive; the redox potential of the ferrocene derivatives can be tuned by the introduction of functional groups or by changing the matrix to host it.[58,59]

CONCLUSIONS

The electrospun fibers of ferrocene-containing pyrazoline derivatives with PMCh/PET were obtained successfully via an electrospinning method, and the fiber morphology exhibited regular formation. CV results were recorded in the presence of ferrocene in PB. These results were not dependent on the skeletal structure of the PMCh/PET electrospun fibers. For the PMCh/PET/Fc-1 electrospun fibers, the oxidation potential increased with increasing phosphate concentration. The results serve to underscore new recognition motifs in the design of ferrocene-containing pyrazoline derivatives as anionic sensors, and the design based on this article can be further modified to construct promising systems for different applications (e.g., drug–polymer compatibility studies).

REFERENCES

1. Arrayás, R. G.; Adrio, J.; Carretero, J. C. *Angew. Chem. Int. Ed.* **2006**, *45*, 7674.
2. Deng, K.; Zhou, J.; Li, X. *Electrochim. Acta* **2013**, *95*, 18.
3. Togni, A.; Hayashi, T. Ferrocenes: Homogeneous Catalysis, Organic Synthesis, Material Science; Wiley-VCH: Weinheim, **1995**.
4. Stepnicka, P. Ferrocenes: Ligands, Materials and Biomolecules; Wiley: Hoboken, NJ, **2008**.
5. Kumar, C. K.; Trivedi, R.; Kumar, K. R.; Giribabu, L.; Sridhar, B. J. *Organomet. Chem.* **2012**, *718*, 64.
6. Zapata, F.; Caballero, A.; Espinosa, A.; Tárraga, A.; Molina, P. *Dalton Trans.* **2010**, *39*, 5429.
7. Khramov, D. M.; Boydston, A. J.; Bielawski, C. W. *Angew. Chem. Int. Ed.* **2006**, *45*, 6186.
8. Romero, T.; Caballero, A.; Tárraga, A.; Molina, P. *Org. Lett.* **2009**, *11*, 3466.
9. Tropiano, M.; Kilah, N. L.; Morten, M.; Rahman, H.; Davis, J. J.; Beer, P. D.; Faulkner, S. *J. Am. Chem. Soc.* **2011**, *133*, 11847.
10. Ganesh, V.; Sudhir, V. S.; Kundu, T.; Chandrasekaran, S. *Chem. Asian J.* **2011**, *6*, 2670.
11. Trivedi, R.; Deepthi, S. B.; Giribabu, L.; Sridhar, B.; Sujitha, P.; Kumar, C. G.; Ramakrishna, K. V. S. *Eur. J. Inorg. Chem.* **2012**, *2012*, 2267.
12. Otón, F.; Espinosa, A.; Tárraga, A.; de Arellano, C. R.; Molina, P. *Chem. Eur. J.* **2007**, *13*, 5742.
13. Dai, L.-X.; Tu, T.; You, S.-L.; Deng, W.-P.; Hou, X.-L. *Acc. Chem. Res.* **2003**, *36*, 659.
14. Anderson, C. E.; Donde, Y.; Douglas, C. J.; Overman, L. E. *J. Org. Chem.* **2005**, *70*, 648.
15. Parveen, H.; Hayat, F.; Salahuddin, A.; Azam, A. *Eur. J. Med. Chem.* **2010**, *45*, 3497.
16. Song, H.; Li, X.; Long, Y.; Schatte, G.; Kraatz, H.-B. *Dalton Trans.* **2006**, *39*, 4696.
17. Horikoshi, R.; Nambu, C.; Mochida, T. *New J. Chem.* **2004**, *28*, 26.
18. Van Staveren, D. R.; Metzler-Nolte, N. *Chem. Rev.* **2004**, *104*, 5931.

19. Bostancıoğlu, R. B.; Demirel, S.; Turgut Cin, G.; Koparal, A. T. *Drug Chem. Toxicol.* **2013**, *36*, 484.
20. Schmittel, M.; He, B.; Kalsani, V.; Bats, J. W. *Org. Biomol. Chem.* **2007**, *5*, 2395.
21. Sun, H.; Steeb, J.; Kaifer, A. E. *J. Am. Chem. Soc.* **2006**, *128*, 2820.
22. Zandler, M. E.; Smith, P. M.; Fujitsuka, M.; Ito, O.; D'Souza, F. *J. Org. Chem.* **2002**, *67*, 9122.
23. Perez, L.; El-Khouly, M. E.; de la Cruz, P.; Araki, Y.; Ito, O.; Langa, F. *Eur. J. Org. Chem.* **2007**, *2007*, 2175.
24. Molina, P.; Tárraga, A.; Caballero, A. *Eur. J. Inorg. Chem.* **2008**, *2008*, 3401.
25. Bian, B.; Ji, S. J.; Shi, H. B. *Dyes Pigments* **2008**, *76*, 348.
26. Lu, Z.; Jiang, Q.; Zhu, W.; Xie, M.; Hou, Y.; Chen, X.; Wang, Z. *Synth. Met.* **2000**, *111*, 465.
27. Li, J. F.; Guan, B.; Li, D. X.; Dong, C. *Spectrochim. Acta* **2007**, *68*, 404.
28. Wang, P.; Onozawa-Komatsuzaki, N.; Himeda, Y.; Sugihara, H.; Arakawa, H.; Kasuga, K. *Tetrahedron Lett.* **2001**, *42*, 9199.
29. De Silva, A. P.; Gunaratne, H. Q.; Gunnlaugsson, T.; Huxley, A. J.; McCoy, C. P.; Rademacher, J. T.; Rice, T. E. *Chem. Rev.* **1997**, *97*, 1515.
30. Zhenglin, Y.; Shikang, W. J. *Lumin.* **1993**, *54*, 303.
31. Gong, Z.-L.; Zhao, B.-X.; Liu, W.-Y.; Lv, H.-S. *J. Photochem. Photobiol. A* **2011**, *218*, 6.
32. Doroshenko, A. O.; Skripkina, V. T.; Schershukov, V. M.; Ponomaryov, O. A. *J. Fluoresc.* **1997**, *7*, 131.
33. Gong, Z.-L.; Xie, Y.-S.; Zaho, B.-X.; Lv, H.-S.; Liu, W.-Y.; Zheng, L.-W.; Lian, S. J. *Fluoresc.* **2011**, *21*, 355.
34. Liu, W.-Y.; Xie, Y.-S.; Zaho, B.-X.; Wang, B.-S.; Lv, H.-S.; Gong, Z.-L.; Lian, S.; Zheng, L.-W. *J. Photochem. Photobiol. A* **2010**, *214*, 135.
35. Ratković, Z.; Juranić, Z. D.; Stanojković, T.; Manojlović, D.; Vukićević, R. D.; Radulović, N.; Joksović, M. D. *Bioorg. Chem.* **2010**, *38*, 26.
36. Turgut Cin, G.; Demirel Topel, S.; Cakıcı, A.; Özek Yıldırım, A.; Karadağ, A. *J. Chem. Crystallogr.* **2012**, *42*, 372.
37. Yılmaz, Ö; Odacı Demirkol, D.; Gülcemal, S.; Kılınç,, A.; Timur, S.; Çetinkaya, B. *Colloids Surf. B* **2012**, *100*, 62.
38. Saleem, M.; Yu, H.; Wang, L.; Abdin, Z.; Khalid, H.; Akram, M.; Abbasi, N. M.; Huang, J. *Anal. Chim. Acta* **2015**, *876*, 9.
39. Chronakis, I. S.; Grapenson, S.; Jakob, A. *Polymer* **2006**, *47*, 1597.
40. Jung, K. H.; Huh, M. W.; Meng, W.; Yuan, J.; Hyun, S. H.; Bae, J. S.; Hudson, S. M.; Kang, I. K. *J. Appl. Polym. Sci.* **2007**, *105*, 2816.
41. Chai, J. H.; Wu, Q. S. *Beilstein J. Nanotechnol.* **2013**, *4*, 189.
42. Nohut Maslakci, N.; Kiristi, M.; Kuralay, F.; Oksuz, L.; Uygun Oksuz, A. J. *Inorg. Organomet. Polym.* **2015**, *25*, 544.
43. Ignatova, M.; Manolova, N.; Rashkov, I. *Macromol. Biosci.* **2013**, *13*, 860.
44. Sun, K.; Li, Z. H. *Express Polym. Lett.* **2011**, *5*, 342.
45. Pakravan, M.; Heuzey, M. C.; Ajji, A. *Biomacromolecules* **2012**, *13*, 412.
46. Kiristi, M.; Uygun Oksuz, A.; Oksuz, L.; Ulusoy, S. *Mater. Sci. Eng. C* **2013**, *33*, 3845.
47. Uygun, A.; Kiristi, M.; Oksuz, L.; Manolache, S.; Ulusoy, S. *Carbohydr. Res.* **2011**, *346*, 259.
48. Karadayı, N.; Turgut Cin, G.; Demirel, S.; Çakıcı, A.; Büyükgüngör, O. *Acta Crystallogr. Sect. E* **2009**, *65*, 127.
49. Veleirinho, B.; Rei, M. F.; Lopes-Da-Silva, J. A. *J. Polym. Sci. Part B: Polym. Phys.* **2008**, *46*, 460.
50. Saïed, N.; Aïder, M. *J. Food Res.* **2014**, *3*, 71.
51. Bhardwaj, N.; Kundu, S. C. *Biotechnol. Adv.* **2010**, *28*, 325.
52. Eren, E.; Aslan, E.; Uygun Oksuz, A. *Polym. Eng. Sci.* **2014**, *54*, 2632.
53. Torres-Huerta, A. M.; Palma-Ramírez, D.; Domínguez-Crespo, M. A.; Del Angel-López, D.; de la Fuente, D. *Eur. Polym. J.* **2014**, *61*, 285.
54. Batterjee, S. M.; Marzouk, M. I.; Aazab, M. E.; El-Hashash, M. A. *Appl. Organomet. Chem.* **2003**, *17*, 291.
55. Satheshkumar, A.; Manivannan, R.; Elango, K. P. J. *Organomet. Chem.* **2014**, *750*, 98.
56. Hendsbee, A. D.; Sun, J. P.; McCormick, T. M.; Hill, I. G.; Welch, G. C. *Org. Electron.* **2015**, *18*, 118.
57. Gündogan-Paul, M.; Özyörük, H.; Çelebi, S. S.; Yildiz, A. *Electroanalysis* **2002**, *14*, 505.
58. Nagarale, R. K.; Lee, J. M.; Shin, W. *Electrochim. Acta* **2009**, *54*, 6508.
59. Chen, J.; Burrell, A. K.; Collis, G. E.; Officer, D. L.; Swiegers, G. F.; Too, C. O.; Wallace, G. G. *Electrochim. Acta* **2002**, *47*, 2715.